Seasonality and trends of snow-cover, vegetation index, and temperature in northern Eurasia

Dennis G. Dye
Ecosystem Change Research Program, Frontier Research System for Global Change, Yokohama, Japan

Compton J. Tucker
Laboratory for Terrestrial Physics, NASA Goddard Space Flight Center, Maryland, USA

Received 3 October 2002; revised 7 February 2003; accepted 5 March 2003; published 11 April 2003.

[1] We examine seasonal variability in snow-cover, normalized difference vegetation index (NDVI), and temperature in a broad region of northern Eurasia, and the spatial and temporal correspondence among trends in these variables between 1982 and 1999. Our results support the contention that the previously reported springtime "greening" trend in northern Eurasian land areas arises from a combination of: (1) the direct effects of declining snow-cover on surface spectral reflectance and NDVI, and (2) enhanced vegetation growth and green biomass stimulated by warmer air temperatures and potentially greater vegetation absorption of photosynthetically active radiation (PAR) during the period of annual peak solar irradiance. *INDEX TERMS:* 1620 Global Change: Climate dynamics (3309); 1615 Global Change: Biogeochemical processes (4805); 0315 Atmospheric Composition and Structure: Biosphere/atmosphere interactions; 1863 Hydrology: Snow and ice (1827); 1640 Global Change: Remote sensing. **Citation:** Dye, D. G., and C. J. Tucker, Seasonality and trends of snow-cover, vegetation index, and temperature in northern Eurasia, *Geophys. Res. Lett.*, *30*(7), 1405, doi:10.1029/2002GL016384, 2003.

1. Introduction

[2] A combination of observational and modeling studies have reported and affirmed that vegetation growth activity in high northern land areas increased over recent decades [*Lucht et al.*, 2002; *Zhou et al.*, 2001]. The northern greening trend is evident in time-series data of the normalized difference vegetation index (NDVI) collected by the Advanced Very High Resolution Radiometer (AVHRR), after corrections for sensor- and atmosphere-related artifacts [*Zhou et al.*, 2001]. The unique spectral reflectance and absorptance characteristics of green leaves cause the NDVI to be sensitive to variations in biophysical attributes of an observed land area (e.g., green biomass and leaf area index) [*Myneni et al.*, 1995]. The factors that underlie the NDVI-inferred northern greening trend have only recently begun to be identified. The trend has been generally explained as a positive response of vegetation growth to higher air temperatures [*Lucht et al.*, 2002; *Zhou et al.*, 2003]. However, increasing temperatures have also been linked to trends toward reduced annual extent and earlier springtime disappearance of snow-cover in northern land areas [*Groisman et al.*, 1994; *Dye*, 2002].

0094-8276/03/2002GL016384$05.00

[3] The high spectral albedo of snow will generally cause the NDVI of a snow-covered vegetation landscape to be lower than the value for snow-free conditions. The NDVI measured by the AVHRR would therefore tend to increase as the fraction of snow-covered land area within the sensor's instantaneous field of view (single pixel) decreases (Figure 1). Thus, declining snow-cover may be at least partially responsible for the higher NDVI values associated with the greening trend [*Shabanov et al.*, 2002]. To improve understanding of the environmental factors that underlie the satellite-observed northern greening trend, we examine seasonal variability in snow-cover, NDVI, and air temperature and the spatial and temporal correspondence among recent (1982–1999) trends in these variables in a broad region of northern Eurasia.

2. Data and Methods

2.1. Study Area and Spatial Scale of the Analysis

[4] We examine recent (1982 to 1999) trends in spatial averages of snow-cover, NDVI and air temperature for contiguous 1-degree latitudinal bands across northern Eurasia at latitudes between 50 and 71 degrees north (Figure 2). The study area is within the domain in which snow-cover was observed in every spring and autumn season during the study period as determined in earlier work [*Dye*, 2002].

2.2. Data Sources

2.2.1. Satellite Snow-Cover

[5] We use the data set of weekly Northern Hemisphere snow-cover extent produced by the National Oceanic and Atmospheric Administration (NOAA) from visible-band satellite observations, with corrections applied by D. Robinson (Rutgers Univ.). The spatial resolution varies from about 120 km at low latitudes to roughly 200 km near the poles. The procedure to produce the data is summarized by *Dye* [2002]. The snow-cover data are considered reliable for broad-scale climate studies [*Robinson et al.*, 1995], but may be less reliable for analysis at the scale of individual grid cells. We address this limitation by performing our analysis at the zonal scale (1 degree latitudinal bands). For each week and latitude, we compute the zonal fraction of snow-free land (ZFSF) as the ratio of the number of snow-free grid cells to the total number of grid cells in the latitude band. We simulate a daily resolution by assuming ZFSF varies linearly between the central days of consecutive weeks.

2.2.2. Satellite NDVI

[6] We use the NDVI data set for the Eurasian continent produced from AVHRR observations by the Global Inven-

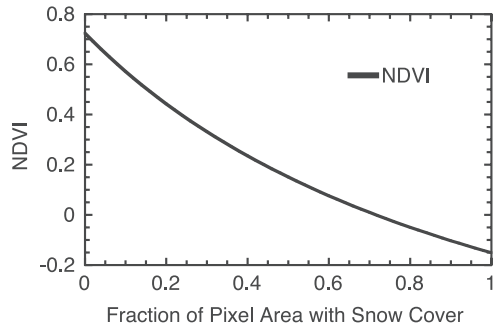

Figure 1. Relationship between fractional snow-cover area and NDVI for a satellite-observed green vegetation landscape (pixel) as predicted by linear spectral mixture modeling. The model employed representative values of visible and near-infrared surface reflectance for pure samples of snow and dense green vegetation.

tory, Monitoring and Modeling Studies (GIMMS) group at NASA Goddard Space Flight Center, Maryland, USA [*Zhou et al.*, 2003]. Atmospheric effects were reduced by adopting the maximum-value NDVI composite procedure, in which only the maximum NDVI value observed at a given pixel location within each consecutive 15-day period is retained for analysis [*Zhou et al.*, 2003]. The NDVI data have a spatial resolution of 8 km. Details of the GIMMS NDVI data set are described by *Zhou et al.* [2001, 2003].

[7] We compute the zonal mean NDVI (ZND) for pixels within contiguous 1-degree latitudinal bands across the study domain. For each time period t, we normalize ZND to the mean annual ZND range for each latitude l. This normalized value, ZNDN, is computed as

$$\mathrm{ZNDN}_{t,l} = \left(\mathrm{ZND}_{t,l} - \mathrm{ZND}_{\min,l}\right) / \left(\mathrm{ZND}_{\max,l} - \mathrm{ZND}_{\min,l}\right) \quad (1)$$

where $\mathrm{ZND}_{\min}$ and $\mathrm{ZND}_{\max}$ are the 18-year (1982–1999) means of the annual minimum ZND and annual maximum ZND, respectively. We simulate a daily resolution by assuming ZNDN varies linearly between the central days of consecutive 15-day composite periods.

2.2.3. Air Temperature

[8] We use the daily mean above-ground (2 m) air temperature data produced by the NCEP-NCAR Reanalysis Project [*Kalnay*, 1996]. The data are compiled globally on a gaussian grid, with a resolution of approximately 1.9 × 1.9 degrees. We use bilinear interpolation to resample the data to a 1 × 1 degree grid. To reduce noise associated with short-term weather variability, we compute the 10-day running mean temperature, and assign the result to the last day of each 10-day sequence. We then compute daily, zonal means of temperature (ZT) for each 1-degree latitude band in the study domain. For comparison with seasonal changes in ZFSF and ZNDN, we normalize the daily ZT to the 18-year mean of the annual maximum range of daily ZT above 0 degrees C, the result of which we refer to as ZTN.

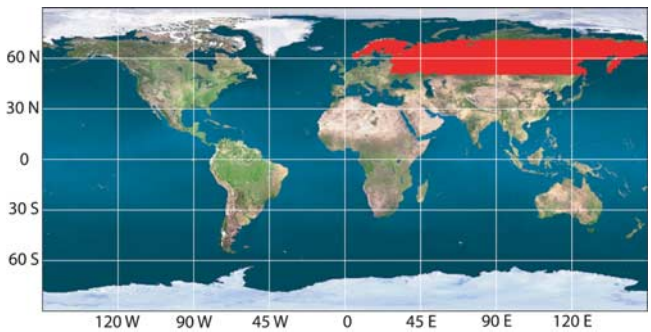

Figure 2. Spatial extent of the northern Eurasia study region (in red).

2.3. Statistical Analysis

[9] The procedures described above produced for each 1-degree latitude band an 18-year time series of daily values of ZFSF, ZNDN, ZT, and ZTN. To characterize seasonal patterns, we compute the 18-year mean of ZFSF, ZNDN, and ZT for each day and latitude band. For each day, we apply least-squares linear regression to the 18-year time series of daily values of ZFSF, ZNDN, and ZT, respectively, to quantify interannual trends. We compute the P-value for the coefficient of each linear equation to assess the statistical confidence of the observed trends.

3. Results and Discussion

3.1. Mean Patterns of Seasonality

[10] The latitude-dependence of the onset and cessation of the active growing season is apparent in the patterns of seasonal change in snow-free status, land surface greenness,

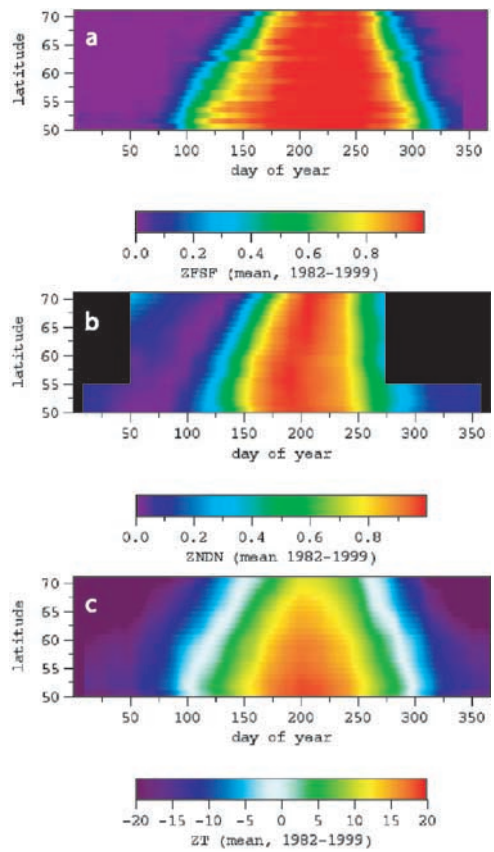

Figure 3. Seasonal variation in zonal (a) snow-cover (ZFSF), (b) normalized NDVI (ZNDN), and (c) air temperature (ZT). All data shown represent mean values for 1982 to 1999.

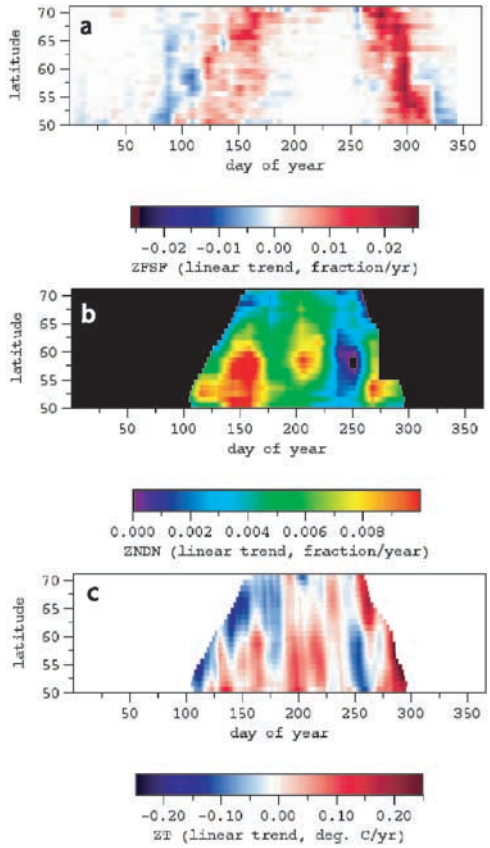

Figure 4. Linear trends (1982–1999) in (a) zonal snow-cover (ZFSF), (b) normalized NDVI (ZNDN), and (c) air temperature (ZT). For ZNDN and ZT, only active growing season values are displayed (defined as days in which the 18-year mean ZT > 0 degrees C).

and air temperature (as indicated by ZFSF, ZNDN and ZT, respectively) (Figure 3). As latitude increases, the timing of the springtime rise of these variables shifts to later dates, while their autumn decline shifts to earlier dates. In contrast to ZFSF and ZT (Figures 3a and 3c), the autumn decline of ZNDN exhibits a relatively weak dependence on latitude (Figure 3b). This pattern suggests an abrupt, near-simultaneous 'shut-down' of vegetation activity in autumn across these north Eurasian land areas.

3.2. Temporal Trends

[11] The spatial patterns of temporal trends for ZFSF, ZNDN, and ZT are displayed in Figure 4, and corresponding *P* values are shown in Figure 5. Trends toward reduced snow-cover are apparent across all latitudes in both spring and autumn (Figure 4a). This result is consistent with previous studies that report a decline in the annual spatial extent and earlier springtime disappearance of snow-cover in Northern Hemisphere land areas [*Groisman et al.*, 1994; *Dye*, 2002].

[12] The ZNDN exhibits positive trends that vary with time and latitude (Figure 4b). The high-latitude "greening" trend has been previously reported on the basis of time-averages of NDVI for monthly and growing-season periods [e.g., *Zhou et al.*, 2001]. We observe intra-seasonal and latitudinal variation in NDVI trends (displayed as ZNDN trends in Figure 4b) that are not apparent in previous studies.

[13] Air temperature (ZT) exhibits a spatially coherent mosaic of positive and negative trends (Figure 4c). Positive temperature trends generally correspond to positive ZNDN trends (Figure 4b). This result is consistent with results of *Zhou et al.* [2003], which indicate warmer temperatures are a primary causal factor for the high latitude greening.

[14] The trends toward reduced snow-cover evident in Figure 4a are consistent with the contention that declining snow cover is a significant causal factor behind the rising trends of ZNDN observed during the early (spring) and late (autumn) periods of the active growing season [*Shabanov et al.*, 2002].

[15] Observation data presented by *Groisman and Davies* [2001] indicate that atmospheric humidity and cloudiness are typically greater over snow-covered land than over snow-free land. Water vapor and clouds tend to reduce the satellite-observed NDVI relative to clear and dry atmospheric conditions. The NDVI composite procedure is expected to minimize such effects, but residual effects cannot be ruled out. Any reduction in humidity or cloudiness that might accompany the trend toward earlier spring snowmelt or later snow-cover onset in autumn, if not adequately accounted for in the AVHRR data processing, could potentially contribute to rising trends in NDVI and ZNDN. Nevertheless, such an artifact would not negate the role of snow-cover and temperature that is suggested by Figure 4.

[16] The positive trends in ZNDN are more pronounced and extensive in spring (approximately days 110 to 175)

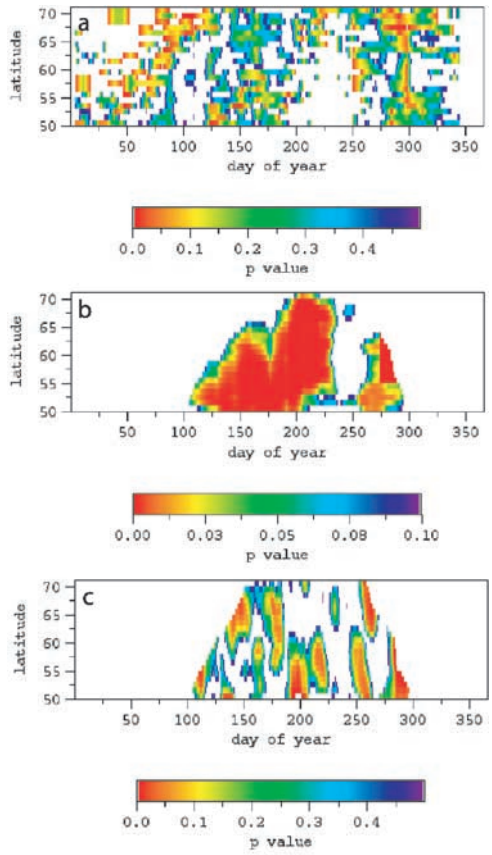

Figure 5. *P* values for the coefficient of the linear trend equations represented in Figure 4 for (a) ZFSF, (b) ZNDN, and (c) ZT.

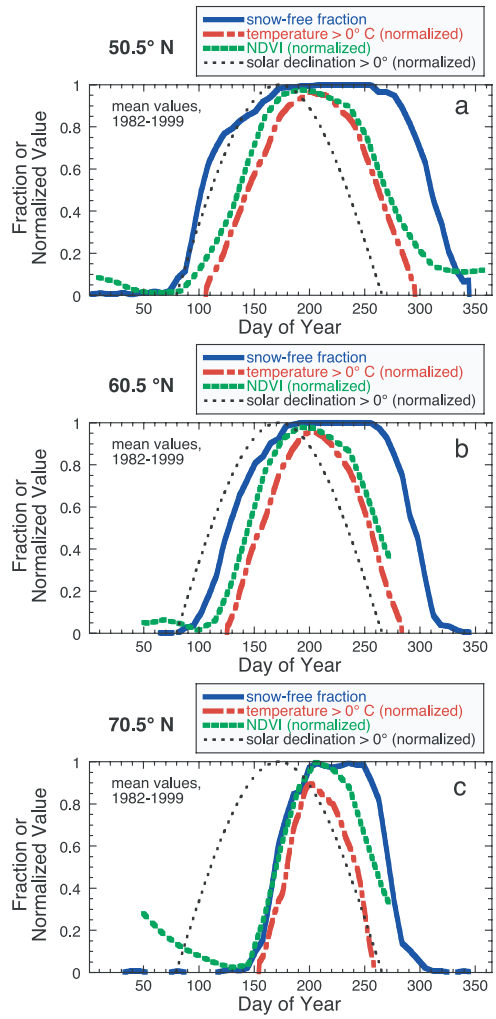

Figure 6. Seasonal variation in daily zonal snow-cover (ZFSF), normalized NDVI (ZNDN), normalized temperature (ZTN), and solar declination for three sample latitudes (a) 50.5 degrees N, (b) 60.5 degrees N, and (c) 70.5 degrees N. All data shown represent the mean values for years 1982 to 1999.

than near the end of the growing season in autumn (approximately days 260 to 290) (Figure 4b). The apparent difference between the spring and autumn responses of vegetation to declining snow-cover may be attributable to seasonal differences in the availability of photosynthetically active radiation (PAR). Snowmelt at high latitudes occurs near the summer solstice when daily PAR and photoperiod are near their annual maximum, as inferred from seasonal variation in solar declination (Figure 6). From an energetics standpoint, a shift toward earlier spring snowmelt would have a greater influence on photosynthetic activity than an equivalent delay in snow cover onset in autumn. Such a seasonal contrast in ecosystem response is generally consistent with the pattern of ZNDN trends observed in Figure 4b, and with evidence from the atmospheric CO_2 record [*Keeling et al.*, 1996] and a process model of terrestrial ecosystem-atmosphere carbon exchange [*Randerson et al.*, 1999].

4. Conclusions

[17] Our analysis reveals new details of seasonal and latitudinal variation in the reported greening trend of north Eurasian land areas, and their relation to trends in snow-cover and air temperature. The results support the contention that the greening trend (rising ZNDN values) that dominates during spring and the early part of the active growing season in northern Eurasia arises from a combination of at least two major factors:

[18] 1. the direct effects of declining snow-cover on surface spectral reflectance, which cause the NDVI to rise [*Shabanov et al.*, 2002], and

[19] 2. enhanced vegetation growth and green biomass production induced by warmer air temperatures (at least partially associated with (1.)) [*Shabanov et al.*, 2002; *Zhou et al.*, 2001, 2003] and increased capture by vegetation of the abundant PAR received during the spring snowmelt season. A quantitative determination of the respective contributions of the above factors to the northern greening trend presents a challenge for future research.

References

Dye, D. G., Interannual variability and trends in the annual snow-cover cycle in Northern Hemisphere land areas, 1972–2000, *Hydrological Proc.*, *16*, 3065–3077, 2002.

Fan, S., M. Gloor, J. Mahlman, S. Pacala, J. Sarmiento, T. Takahashi, and P. Tans, A large terrestrial carbon sink in North America implied by atmospheric and oceanic carbon dioxide data and models, *Science*, *282*, 442–446, 1998.

Groisman, P. Y., T. R. Karl, R. W. Knight, and G. L. Stenchikov, Changes of snow-cover, temperature, and radiative heat balance over the Northern Hemisphere, *J. Climate*, *7*, 1633–1656, 1994.

Groisman, P. Y., and T. D. Davies, Snow cover and the climate system, in *Snow Ecology*, edited by H. G. Jones et al., pp. 1–44, Cambridge Univ. Press, New York, 2001.

Kalnay, E., The NCEP/NCAR 40-year reanalysis project, *Bull. Am. Meteor. Soc.*, *77*, 437–471, 1996.

Keeling, C. D., J. F. S. Chin, and T. P. Whorf, Increased activity of northern vegetation inferred from CO_2 measurements, *Nature*, *382*, 146–149, 1996.

Lucht, W., I. C. Prentice, R. B. Myneni, S. Sitch, P. Friedlingstein, W. Cramer, P. Bousquet, W. Buermann, and B. Smith, Climatic control of the high-latitude vegetation greening trend and Pinatubo effect, *Science*, *296*, 1687–1688, 2002.

Myneni, R. B., F. G. Hall, P. J. Sellers, and A. L. Marshak, The interpretation of spectral vegetation indexes, *IEEE Trans. Geosci. Remote Sens.*, *33*, 481–486, 1995.

Randerson, J. T., C. B. Field, I. Y. Fung, and P. P. Tans, Increases in early season ecosystem uptake explain recent changes in the seasonal cycle of atmospheric CO_2 at high northern latitudes, *Geophys. Res. Lett.*, *26*, 2765–2768, 1999.

Robinson, D. A., A. Frei, and M. C. Serreze, Recent variations and regional relationships in Northern Hemisphere snow cover, *Ann. Glaciology*, *21*, 71–76, 1995.

Shabanov, N. V., L. Zhou, Y. Knyazikhin, R. B. Myneni, and C. J. Tucker, Analysis of interannual changes in northern vegetation activity observed in AVHRR data from 1981 to 1994, *IEEE Trans. Geos. Rem. Sens.*, *40*, 115–130, 2002.

Zhou, L., C. J. Tucker, R. K. Kaufmann, D. Slayback, N. V. Shabonaov, and R. B. Myneni, Variations in northern vegetation activity inferred from satellite data of vegetation index during 1981 to 1999, *J. Geophys. Res.*, *106*(D1), 20,069–20,083, 2001.

Zhou, L., R. K. Kaufmann, Y. Tian, R. B. Myneni, and C. J. Tucker, Relation between interannual variations in satellite measures of northern forest greenness and climate between 1982 and 1999, *J. Geophys. Res.*, *108*(D1), doi: 10.1029/2002JD002510, 2003.

D. G. Dye, FRSGC, 3173-25 Showa-machi, Kanazawa-ku, Yokohama, Kanagawa-ken, 236-0001, Japan. (dye@jamstec.go.jp)

C. J. Tucker, Code 923, NASA/GSFC, Greenbelt, MD 20771, USA.